Flexible Active Power Control of Distributed Power Generation Systems During Grid Faults

Pedro Rodriguez, *Member, IEEE*, Adrian V. Timbus, *Student Member, IEEE*, Remus Teodorescu, *Senior Member, IEEE*, Marco Liserre, *Senior Member, IEEE*, and Frede Blaabjerg, *Fellow, IEEE*

***Abstract*—The increasing penetration of distributed power generation into the power system leads to a continuous evolution of grid interconnection requirements. In particular, active power control will play an important role both during grid faults (low-voltage ride-through capability and controlled current injection) and in normal conditions (reserve function and frequency regulation). The aim of this paper is to propose a flexible active power control based on a fast current controller and a reconfigurable reference current selector. Several strategies to select the current reference are studied and compared using experimental results that are obtained during an unsymmetrical voltage fault. The results of the analysis allow selection of the best reference current in every condition. The proposed methods facilitate multiple choices for fault ride through by simply changing the reference selection criteria.**

***Index Terms*—Control strategies, distributed power generation systems (DPGSs), fault ride through, grid faults, positive and negative sequences, power control, wind turbines (WTs).**

I. Introduction

In THE last decade, distributed power generation systems (DPGSs) based on renewable energies contribute more and more to the total amount of energy production on the globe. Wind turbines (WT) as well as photovoltaic (PV) systems are seen as reliable energy sources that should be further exploited in order to achieve maximum efficiency and overcome the increasing power demand in the world. These systems are no longer regarded as engineering issues, but they are widely recognized as reliable systems, which can have a large share in energy production in the future.

The possibility of energy production using a clean technology makes both WT and PV systems very attractive, but the control of these systems is a challenge due to the uncertainty in the availability of the input power [1]. Moreover, the increased amount of distributed systems that are connected to the utility network can create instability in the power systems, even leading to outages.

In order to maintain a stable power system in countries with a large penetration of distributed power, transmission system operators issue more stringent demands regarding the interconnection of the DPGS to the utility grid [2]–[4]. Among the new demands, power generation systems are requested to ride through grid disturbances and to provide ancillary services in order to behave as a conventional power plant, and hence to have the capability of sustaining the utility network in the situation of a fault. Therefore, the grid fault influence on the control of DPGS needs to be investigated.

This paper discusses some possible control strategies that a DPGS can adopt when running on faulty grid conditions. First, a classification of the grid faults is presented, followed by some consideration of the control strategy when an unbalanced fault takes place in the grid. Then, the control strategies that are investigated are further described, followed by the presentation of the algorithm that is used for detecting the positive and negative sequences of the grid voltage. Finally, experimental results are presented in order to verify the theory of each control strategy.

II. Grid Fault Considerations

Input power variations due to meteorological conditions and grid-voltage variation due to connection and disconnection of loads challenge the ability of WTs to provide constant output power at the point of common coupling (PCC). Investigations for compensating these oscillations using different energy storage systems such as flywheels [5], [6] or appealing to power quality compensation units such as dynamic voltage restorers [7], [8] have been investigated. One of the newly introduced requests for interconnecting WT systems to the utility network is stressing their ability to ride through short grid disturbances, such as voltage and frequency variations [3], [4]. As a consequence, the low-voltage ride-through feature of WT systems has become of high interest nowadays.

With respect to the grid-voltage variation, the grid faults can be classified in two main types [9].

1) *Balanced fault:* when all three grid voltages register the same drop/swell amplitude but the system remains balanced. The occurrence of this type of fault is extremely rare in power systems.
2) *Unbalanced fault:* when the three grid voltages register unequal drop/swell amplitudes. Usually, phase shift between the phases also appears in this situation. This type

Manuscript received October 5, 2006; revised January 29, 2007. This work was supported in part by the Risø National Lab, Energinet.dk, and the Danish Research Council under Contract 2058-03-0003 and in part by the Ministerio de Ciencia y Tecnologia of Spain under Project ENE2004-07881-C03-02.

P. Rodriguez is with the Department of Electrical Engineering, Technical University of Catalonia, 08222 Barcelona, Spain (e-mail: prodriguez@ee.upc.edu).

A. V. Timbus, R. Teodorescu, and F. Blaabjerg are with the Institute of Energy Technology, Aalborg University, 9220 Aalborg, Denmark (e-mail: avt@iet.aau.dk; ret@iet.aau.dk; fbl@iet.aau.dk).

M. Liserre is with the Department of Electrotechnical and Electronic Engineering, Politecnico di Bari, 70125 Bari, Italy (e-mail: liserre@ieee.org).

Color versions of one or more of the figures in this paper are available online at http://ieeexplore.ieee.org.

Digital Object Identifier 10.1109/TIE.2007.899914

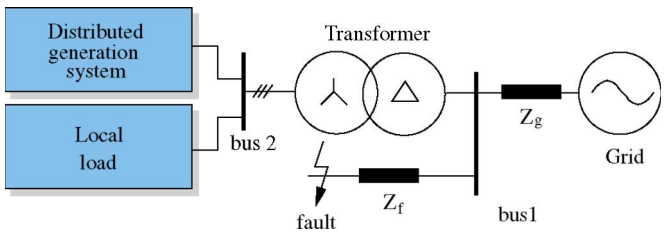

Fig. 1. Distributed generation system that is connected through a Δy transformer to the utility network.

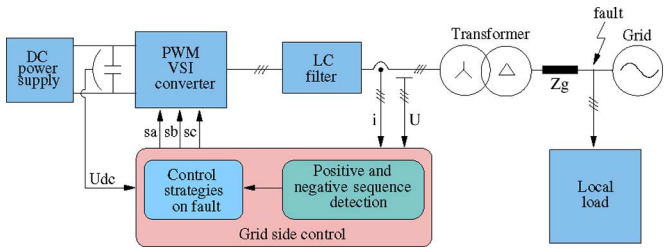

Fig. 2. Diagram of the laboratory setup that is used to test the proposed control strategies when running on faulty grid conditions.

of fault occurs due to one or two phases that are shorted to ground or to each other. In [9] and [10], a detailed description of unbalanced grid faults is given, and five types of unbalanced faults are distinguished. One interesting fact is that the distribution transformer, usually of type Δy, also has influence on how the grid fault appears at DPGS terminals. According to [10], all unbalanced grid faults create both uneven voltage magnitudes and phase angle jumps at DPGS terminals, when such a transformer is used.

For example, considering the DPGS that is connected to the utility network, as shown in Fig. 1, where a distribution transformer is used by the generation system to interface to the utility network, the voltage fault occurring at bus 1 appears different at bus 2. If a severe grid fault like a single phase that is shorted to ground takes place at bus 1, the voltage amplitude at the DPGS terminals (after the transformer) will have a magnitude that is dependent on two impedance values Z_g and Z_f, and the transformer type.

Characteristic to the unbalanced fault is the appearance of the negative-sequence component in the grid voltages. This gives rise to double-frequency oscillations in the system, which are reflected as ripple in the dc-link voltage and output power [11], [12]. Such oscillations can lead to a system trip if the maximum dc-link voltage is exceeded and can also have a negative influence on the control of the grid converter, e.g., producing a nonsinusoidal current reference that considerably deteriorates the power quality and may even trip the overcurrent protections. As a consequence, the influence of grid faults on the control of DPGSs needs to be investigated.

III. Fault Control in Grid and Micro-Grid

Owing to the appearance of a negative sequence and amplitude drop in the grid voltages, the current magnitude that is delivered by the DPGS to the grid will rise considerably for the same amount of delivered power. Moreover, a negative-sequence current will appear, flowing uncontrollably through the power converter of the distribution system. In this sense, in [13], an approach based on a series inverter that is connected at the PCC and controlled as a current limiting impedance is proposed as a solution to limit the current rising inside the microgrid. Additionally, in [14], it is argued that the switching of loads in microgrids can cause relatively high transients in the voltage, and it is suggested that all power generation units should support the grid during such a disturbance in order to return to normal operating conditions. Moreover, the bandwidth of communication signals between the DPGS that is connected to the microgrid proves to be a big impediment for achieving proper implementation of such decentralized control. An improved solution, which bypasses this problem using variations in output impedance of each distributed system, is proposed in [15].

With respect to the negative-sequence current flowing through the grid-connected power converter, in [16] and [17], the implementation of a dual current controller, with one for the positive-sequence current and one for the negative-sequence current, has been discussed, and improved results are noticed when the negative-sequence current is also controlled. It should be noticed here that the complexity of the controller is doubled in this case, and an algorithm for detection of both positive- and negative-sequence components is necessary. As can be observed in [18], the ripple of the dc-link voltage still has influence on the reference currents, leading to nonsinusoidal current injection, but in [19], the authors discuss the possibility of controlling the negative-sequence current in a way that cancels out the oscillation in the dc-link voltage. Again, the positive- and negative-sequence components of the voltage must be identified, but noticeable in this case is the lack of double-frequency oscillations in the dc-link voltage.

This paper investigates the control possibilities of a DPGS when running on unbalanced grid faults. For simplicity, only the grid-side converter is considered here. The input power source and its control are disregarded. Hence, the investigated control strategies can be applied to a variety of DPGSs. Additionally, the dc-link voltage controller is not included in the control strategy. The design of this controller when the DPGS operates on a faulty grid is beyond the purpose of this paper. Fig. 2 depicts a schematic of the proposed control, emphasizing the algorithm for positive- and negative-sequence detection and the control strategy block.

As shown in [20], there are different ways to structure the grid converter control, and here, the implementation in a $\alpha\beta$ stationary reference frame using a dead beat current controller has been selected. The main contribution of this paper is the creation of current references depending on the selected control strategy, as Fig. 3 illustrates.

The next section provides a deep insight into the investigated strategies for generating the current references, and analytical equations are provided and discussed. These strategies can be an add-on feature to the basic control structures of grid-connected power generation systems [20] in order to facilitate different options when running through grid disturbances. As there are five different methods that are derived for generating

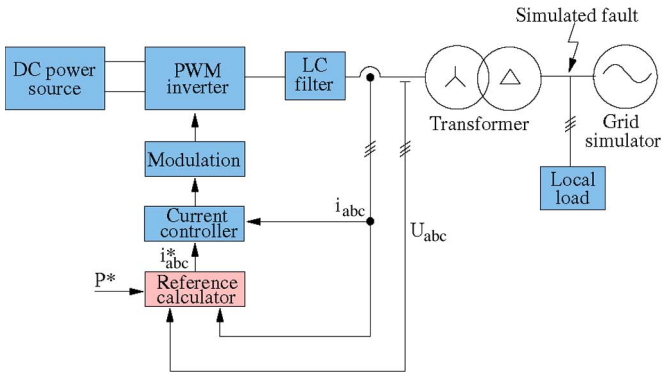

Fig. 3. Schematic of the proposed control structure when DPGS is running on faulty grid conditions.

current references, the work in this paper is limited to active current/power control only, with reactive power control being disregarded [25].

IV. Current Control Strategies When Running on Grid Faults

Instantaneous active power p, which is delivered by a three-phase inverter to the grid, depends on the voltage vector in the PCC $\mathbf{v} = (v_a, v_b, v_c)$ and on the injected current vector in this point $\mathbf{i} = (i_a, i_b, i_c)$, such that

$$p = \mathbf{v} \cdot \mathbf{i} \tag{1}$$

where $\cdot$ represents the dot product. Therefore, for a given voltage vector, there exist infinite current vectors, which are able to deliver exactly the same instantaneous active power to the grid. In this paper, it has been assumed that the energy source supplying power through the inverter exhibits slow dynamics, and hence, the active power reference will be considered a constant throughout each grid-voltage cycle. However, conclusions from this study are also valid for those cases in which the reference for the instantaneous active power could experience oscillations throughout a grid period, e.g., when active filtering functionality is implemented in the inverter.

The next paragraphs propose five different strategies for generating inverter reference currents in order to deliver to the grid active power $p = P^*$. In these strategies, it has been assumed that no reactive power should be injected to the grid ($q^* = 0$).

A. Instantaneous Active Reactive Control (IARC)

The most efficient set of currents delivering instantaneous active power P to the grid can be calculated as follows [21]:

$$\mathbf{i}^*_p = g\mathbf{v}, \qquad \text{with} \quad g = \frac{P}{|\mathbf{v}|^2} \tag{2}$$

where $|\mathbf{v}|$ denotes the module of the three-phase voltage vector $\mathbf{v}$, and g is the instantaneous conductance that is seen from the inverter output. In this situation, the grid converter is controlled to emulate a symmetric resistance on all three phases [22]. The value of g is a constant in balanced sinusoidal conditions, but under grid faults, however, the negative-sequence component gives rise to oscillations at twice the fundamental frequency in $|\mathbf{v}|$. Consequently, the injected currents will not keep their sinusoidal waveform, and high-order components will appear in their waveform. A current vector of (2) is instantaneously proportional to the voltage vector and therefore does not have any orthogonal component in relation to the grid voltage; hence, it gives rise to the injection of no reactive power to the grid.

Instantaneous power theories [21], [23] allow for identifying active and reactive components of the current for power delivery optimization, making reactive currents equal zero. However, when the quality of the current that is injected into the unbalanced grid becomes a major issue, it is necessary to establish certain constraints about what the current sequence components and harmonics should be, even knowing that power delivery efficiency will decrease.

B. Instantaneously Controlled Positive-Sequence (ICPS)

The instantaneous active power that is associated with an unbalanced current $\mathbf{i} = \mathbf{i}^+ + \mathbf{i}^-$, which is injected at the PCC of a three-phase unbalanced grid with $\mathbf{v} = \mathbf{v}^+ + \mathbf{v}^-$, is given by

$$p = \mathbf{v} \cdot \mathbf{i} = \mathbf{v}^+\mathbf{i}^+ + \mathbf{v}^-\mathbf{i}^- + \mathbf{v}^+\mathbf{i}^- + \mathbf{v}^-\mathbf{i}^+ \tag{3}$$

where superscripts "+" and "−" denote the three-phase sinusoidal positive- and negative-sequence signals, respectively. From (3), the positive-sequence current can be instantaneously controlled to deliver active power P by imposing the following constraints in the current reference calculation:

$$\mathbf{v} \cdot \mathbf{i}^{*+}_{\mathbf{p}} = P \tag{4a}$$

$$\mathbf{v} \cdot \mathbf{i}^{*-}_{\mathbf{p}} = 0. \tag{4b}$$

Equation (4b) makes negative-sequence current components equal zero, whereas the positive-sequence current reference can be calculated from (4a) as follows:

$$\mathbf{i}^*_{\mathbf{p}} = \mathbf{i}^{*+}_{\mathbf{p}} + \mathbf{i}^{*-}_{\mathbf{p}} = g^+\mathbf{v}^+ \tag{5a}$$

$$g^+ = \frac{P}{|\mathbf{v}^+|^2 + \mathbf{v}^+ \cdot \mathbf{v}^-}. \tag{5b}$$

According to the p–q theory [21], the instantaneous reactive power that is associated with the current vector of (5a) is given by

$$q = \left|\mathbf{v} \times \mathbf{i}^{*+}_p\right| = \underbrace{\left|\mathbf{v}^+ \times \mathbf{i}^{*+}_p\right|}_{0} + \underbrace{\left|\mathbf{v}^- \times \mathbf{i}^{*+}_p\right|}_{\tilde{q}} \tag{6}$$

where the sign $\times$ denotes the cross product. It is possible to appreciate that the current reference that is calculated by means of (6) gives rise to oscillations at twice the fundamental utility frequency in the instantaneous reactive power that is injected to the grid.

It is worth noticing that positive- and negative-sequence components of the grid voltage should be perfectly characterized to implement this control strategy. Therefore, an algorithm that

is capable of detecting the voltage-sequence components under unbalanced operating conditions should be added to the control system. The description of the algorithm that is used in this paper is further presented in Section V.

C. Positive–Negative-Sequence Compensation (PNSC)

Active power P can be delivered to the grid by injecting sinusoidal positive- and negative-sequence currents at the PCC. To achieve this, the following constraints should be imposed in the current reference calculation:

$$\mathbf{v}^+ \cdot \mathbf{i}_p^{*+} + \mathbf{v}^- \cdot \mathbf{i}_p^{*-} = P \tag{7a}$$

$$\mathbf{v}^+ \cdot \mathbf{i}_p^{*-} + \mathbf{v}^- \cdot \mathbf{i}_p^{*+} = 0. \tag{7b}$$

From (7b), the negative-sequence reference current can be written as

$$\mathbf{i}_p^{*-} = -g^- \mathbf{v}^-, \qquad \text{where} \quad g^- = \frac{\mathbf{v}^+ \cdot \mathbf{i}_p^{*+}}{|\mathbf{v}^+|^2}. \tag{8}$$

Substituting (8) in (7a) and simplifying, the positive-sequence reference current can be calculated by

$$\mathbf{i}_p^{*+} = g^+ \mathbf{v}^+, \qquad \text{with} \quad g^+ = \frac{P}{|\mathbf{v}^+|^2 - |\mathbf{v}^-|^2}. \tag{9}$$

Adding (8) and (9), the final current reference becomes

$$\mathbf{i}_p^* = \mathbf{i}_p^{*+} + \mathbf{i}_p^{*-} = g^{\pm}(\mathbf{v}^+ - \mathbf{v}^-), \tag{10a}$$

$$\text{with} \quad g^{\pm} = \frac{P}{|\mathbf{v}^+|^2 - |\mathbf{v}^-|^2}. \tag{10b}$$

Equation (10a) indicates that the injected current and voltage vectors have different directions. Consequently, the instantaneous reactive power that is delivered to the grid is not equal to zero but exhibits second-order oscillations given by

$$\begin{aligned} q &= \left|\mathbf{v} \times \mathbf{i}_p^*\right| \\ &= \underbrace{\left|\mathbf{v}^+ \times \mathbf{i}_p^{*+}\right| + \left|\mathbf{v}^- \times \mathbf{i}_p^{*-}\right|}_{0} + \underbrace{\left|\mathbf{v}^+ \times \mathbf{i}_p^{*-}\right| + \left|\mathbf{v}^- \times \mathbf{i}_p^{*+}\right|}_{\tilde{q}}. \end{aligned} \tag{11}$$

D. Average Active-Reactive Control (AARC)

During unbalanced grid faults, current references that are obtained by means of the IARC strategy present high-order harmonics in their waveforms because instantaneous conductance g does not remain constant throughout grid period T. Since P has been assumed to be a constant, such harmonics come from the second-order component of $|\mathbf{v}|^2$, being

$$|\mathbf{v}|^2 = |\mathbf{v}^+|^2 + |\mathbf{v}^-|^2 + 2|\mathbf{v}^+||\mathbf{v}^-|\cos(2\omega t + \phi^+ - \phi^-). \tag{12}$$

High-order harmonics in the current references will be canceled if they are calculated by

$$\mathbf{i}_p^* = G\,\mathbf{v}, \qquad \text{where} \quad G = \frac{P}{V_\Sigma^2} \tag{13}$$

where V_Σ is the collective rms value of the grid voltage, and it is defined by

$$V_\Sigma = \sqrt{\frac{1}{T}\int_0^T |\mathbf{v}|^2 dt} = \sqrt{|\mathbf{v}^+|^2 + |\mathbf{v}^-|^2}. \tag{14}$$

In this case, instantaneous conductance is a constant under periodic conditions, namely, $g = G$.

The current vector of (13) has the same direction as the grid-voltage vector, so it will not give rise to any reactive power. However, the instantaneous active power that is delivered to the unbalanced grid will not equal P, but it will be given by

$$p = \mathbf{i}_p^* \cdot \mathbf{v} = \frac{|\mathbf{v}|^2}{V_\Sigma^2} P = P + \tilde{p}. \tag{15}$$

Substituting (12) and (14) in (15), it is easy to justify that the instantaneous active power that is delivered to the unbalanced grid consists of a mean value P that is accompanied by oscillations at twice the grid frequency $\tilde{p}$. Since G is a constant, voltage and current waveforms will be monotonously proportional.

E. Balanced Positive-Sequence Control (BPSC)

When the quality of the currents that are injected in the grid plays a decisive role, they can be calculated as

$$\mathbf{i}_p^* = G^+ \mathbf{v}^+, \qquad \text{where} \quad G^+ = \frac{P}{|\mathbf{v}^+|^2}. \tag{16}$$

The current vector of (16) consists of a set of perfectly balanced positive-sequence sinusoidal waveforms. Under unbalanced operating conditions, the instantaneous active power that is delivered to the grid will differ from P because of the interaction between the positive-sequence injected current and the negative-sequence grid voltage, i.e.,

$$p = \mathbf{v} \cdot \mathbf{i}_p^* = \underbrace{\mathbf{v}^+ \cdot \mathbf{i}_p^*}_{P} + \underbrace{\mathbf{v}^- \cdot \mathbf{i}_p^*}_{\tilde{p}} \tag{17}$$

where $\tilde{p}$ is the power oscillation at twice the fundamental utility frequency. Likewise, the instantaneous reactive power can be calculated as

$$q = \left|\mathbf{v} \times \mathbf{i}_p^*\right| = \underbrace{\left|\mathbf{v}^+ \times \mathbf{i}_p^*\right|}_{0} + \underbrace{\left|\mathbf{v}^- \times \mathbf{i}_p^*\right|}_{\tilde{q}} \tag{18}$$

where $\tilde{q}$ is also oscillating at twice the fundamental utility frequency.

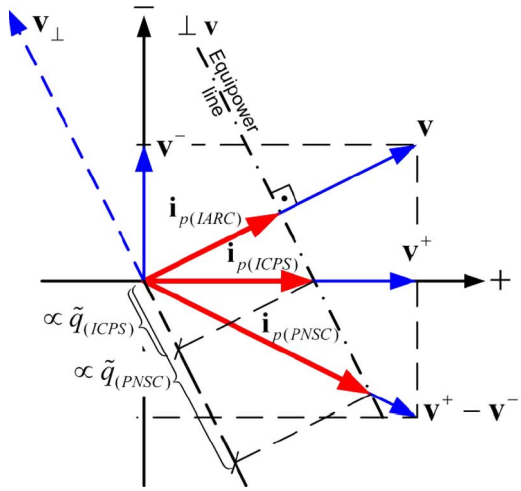

Fig. 4. Graphical representation of voltage and current vectors on a positive–negative-sequence Euclidean plane for different control strategies.

F. Discussion

The positive- and negative-sequence vectors that are studied in this section can be considered to be orthogonal, as seen over one grid period, and represented on a Euclidean plane $\mathbb{R}^2$ since their scalar product throughout the grid period is always equal to zero, i.e.,

$$\overline{\mathbf{x}^+ \cdot \mathbf{y}^-} = \frac{1}{T}\int_0^T \mathbf{x}^+ \cdot \mathbf{y}^- dt = 0. \tag{19}$$

This graphic representation of voltage and current vectors is shown in Fig. 4 and allows better understanding of previous strategies for current reference generation. For better visualization and understanding, only current vectors from the IARC, ICPS, and PNSC strategies have been represented in Fig. 4. The amplitude of all three current vectors is delimited by the *equi-power line*, which is perpendicular to $\mathbf{v}$. The amplitude of oscillations in the instantaneous reactive power that is associated with each strategy $\tilde{q}$ is proportional to the projection of its current vector over the equi-power line. Current vectors from the AARC and BPS strategies have the same direction as those vectors from the IARC and ICPS strategies, respectively. However, their amplitudes are not instantaneously controlled, generating oscillations in the active power. None of these strategies give rise to a finite mean value in the reactive power that is injected to the grid.

V. Detection of Positive and Negative Sequences

Precise characterization of the grid voltage is a crucial issue in order to have full control over the power that is delivered from the DPGS to the grid. In this paper, such characterization is performed by means of a positive–negative-sequence voltage detector based on a second-order generalized integrator (SOGI) [24]. The SOGI diagram is shown in Fig. 5, and its transfer function is given by

$$S(s) = \frac{y}{x}(s) = \frac{\omega_o s}{s^2 + \omega_o^2} \tag{20}$$

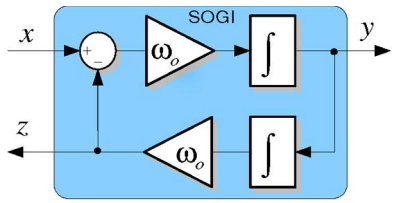

Fig. 5. Structure of the SOGI.

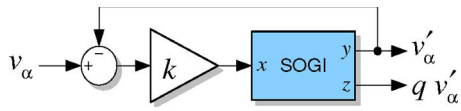

Fig. 6. Structure of a bandpass filter based on SOGI implementation.

where ω_0 is the SOGI resonance frequency. If $x = X\sin(\omega t + \phi)$, the SOGI acts as an ideal integrator when $\omega = \omega_0$. Therefore, the closed-loop diagram that is shown in Fig. 6 gives rise to a second-order bandpass filter (BPF) whose transfer function is

$$V(s) = \frac{v'_\alpha}{v_\alpha}(s) = \frac{k\omega_o s}{s^2 + k\omega_o s + \omega_o^2}. \tag{21}$$

The damping factor of (21) is directly related to the value that is selected for gain k. The system in Fig. 6 exhibits interesting characteristics that make it suitable for grid-voltage characterization.

- If ω_0 and k are properly chosen, v'_α will be almost sinusoidal and will match the fundamental component of v_α.
- Signal qv'_α will be the quadrature-phase version of v_α (90° lagged), which is very useful for the instantaneous detection of symmetrical components in three-phase systems.
- The SOGI resonance frequency can be adjusted by means of the proper phase-locked loop, making the system frequency adaptive [24].

The influence of gain k on the filtering properties of the SOGI system is shown in Fig. 7. As can be noticed, with a lower value of k, the filtering is more tight around the resonance frequency, while a higher value of k permits other frequencies to pass through the filter.

The instantaneous positive- and negative-sequence components $\mathbf{v}^+_{abc}$ and $\mathbf{v}^-_{abc}$, respectively, of a generic voltage vector are given by

$$\mathbf{v}^+_{abc} = [\,v^+_a \quad v^+_b \quad v^+_c\,]^T = [T_+]\mathbf{v}_{abc} \tag{22a}$$

$$\mathbf{v}^-_{abc} = [\,v^-_a \quad v^-_b \quad v^-_c\,]^T = [T_-]\mathbf{v}_{abc} \tag{22b}$$

where $[T_+]$ and $[T_-]$ are defined as

$$[T_+] = \frac{1}{3}\begin{bmatrix} 1 & a & a^2 \\ a^2 & 1 & a \\ a & a^2 & 1 \end{bmatrix} \tag{23a}$$

$$[T_-] = \frac{1}{3}\begin{bmatrix} 1 & a^2 & a \\ a & 1 & a^2 \\ a^2 & a & 1 \end{bmatrix} \tag{23b}$$

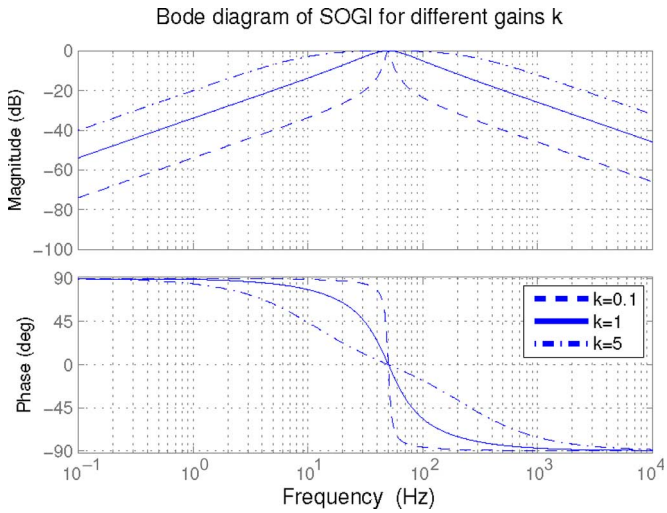

Fig. 7. Bode plot of SOGI–BPF for different values of gain k.

with

$$a = e^{j\frac{2\pi}{3}}.$$

Using the *Clarke* transformation, the voltage vector can be translated from abc to $\alpha\beta$ reference frames as follows:

$$\mathbf{v}_{\alpha\beta} = [\, v_\alpha \quad v_\beta \,]^T = [T_{\alpha\beta}]\, \mathbf{v}_{abc} \tag{24a}$$

$$[T_{\alpha\beta}] = \sqrt{\frac{2}{3}} \begin{bmatrix} 1 & -\frac{1}{2} & -\frac{1}{2} \\ 0 & \frac{\sqrt{3}}{2} & -\frac{\sqrt{3}}{2} \end{bmatrix}. \tag{24b}$$

Therefore, the instantaneous positive- and negative-sequence voltage components on the $\alpha\beta$ reference frame can be calculated as

$$\mathbf{v}^+_{\alpha\beta} = [T_{\alpha\beta}]\mathbf{v}^+_{abc} = [T_{\alpha\beta}][T_+][T_{\alpha\beta}]^T\mathbf{v}_{\alpha\beta} = \frac{1}{2}\begin{bmatrix} 1 & -q \\ q & 1 \end{bmatrix}\mathbf{v}_{\alpha\beta} \tag{25a}$$

$$\mathbf{v}^-_{\alpha\beta} = [T_{\alpha\beta}]\mathbf{v}^-_{abc} = [T_{\alpha\beta}][T_-][T_{\alpha\beta}]^T\mathbf{v}_{\alpha\beta} = \frac{1}{2}\begin{bmatrix} 1 & q \\ -q & 1 \end{bmatrix}\mathbf{v}_{\alpha\beta}$$

$$q = e^{-j\frac{\pi}{2}} \tag{25b}$$

where q is a phase-shift operator in the time domain, which obtains the quadrature-phase waveform (90° lag) of the original in-phase waveform.

Hence, the system that is shown in Fig. 8 is proposed for the detection of the positive and negative sequences on the $\alpha\beta$ reference frame where a SOGI is used to generate the in-phase and quadrature-phase signals of (25a) and (25b).

The proposed positive- and negative-sequence detection system that is exposed in this paper provides an effective solution for grid synchronization of power converters in the presence of grid faults. With proper selection of gain k, SOGI–BPF increases the effectiveness of the detection system when the grid voltage presents high-order harmonics. The calculation of the instantaneous symmetrical components on the $\alpha\beta$ reference frame makes it possible to use only two SOGI–BPFs, which reduces the computational burden of the proposed detection algorithm as compared to the calculations in abc, where three SOGI–BPFs would be necessary.

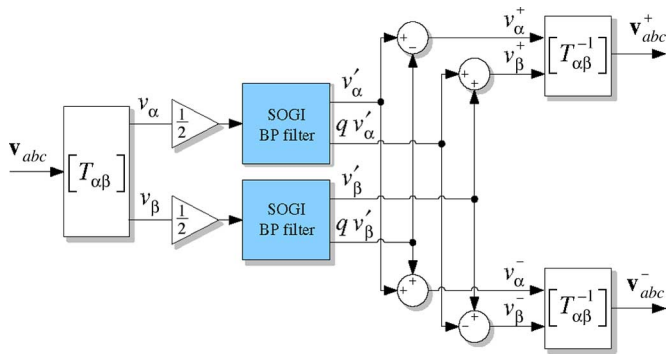

Fig. 8. Proposed structure for extracting the positive and negative sequences of the grid voltages based on SOGI–BPF.

VI. Evaluation of Control Strategies

A. Experimental System

The aforementioned control strategies have been implemented in an experimental setup comprising a pulsewidth-modulation-driven voltage source inverter and an LC filter ($L = 10$ mH and $C = 0.7$ μF per phase) that is connected through a Δy transformer to the grid. The grid is replaced here by a programmable three-phase ac power source, in order to be able to create grid faults. A control structure developed in the stationary reference frame ($\alpha\beta$) using a deadbeat current controller is implemented in a dSpace 1103 card.

Due to the limitation of the ac power source in sinking power, a resistive local load has been connected to the system, as shown in Fig. 2. The dc link voltage controller has been omitted in order not to influence the creation of the current references, and as a consequence, dc power sources are used to supply the necessary dc-link voltage, which is set to 650 V.

B. Fault Conditions

The power system schematic that is illustrated in Fig. 9 has been used as background consideration to obtain a fault condition that can be further used in the laboratory for testing the proposed control strategies.

The DPGS is considered to be connected through a step-up Δy transformer to the medium voltage level (30 kV) at bus 2. The distance between bus 2 and the transmission level of 110 kV is about 10 km. An unbalanced grid fault (single phase to ground) has been considered to occur in bus 2 at a distance of 7.7 km from the PCC. Considering that the characteristic impedance of the power lines in the medium voltage is the same for both 10- and 7.7-km lines, the distance at which the fault is taking place has a major influence on the voltage magnitude at the DPGS terminals.

In the situation of a single-phase-to-ground fault, it can be considered that the current that is injected by the distribution system is considerably smaller as compared to the short circuit current flowing through the faulted line. In this case, the voltage

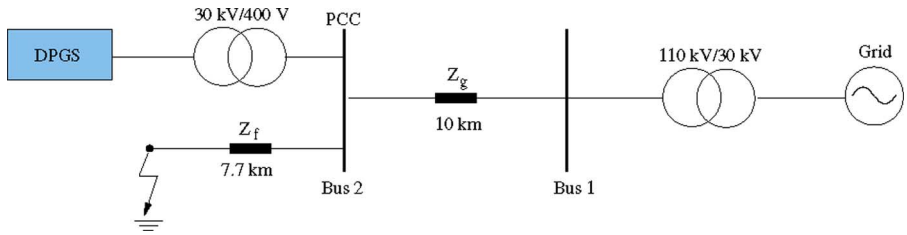

Fig. 9. Power system that is considered to model a single-phase-to-ground fault.

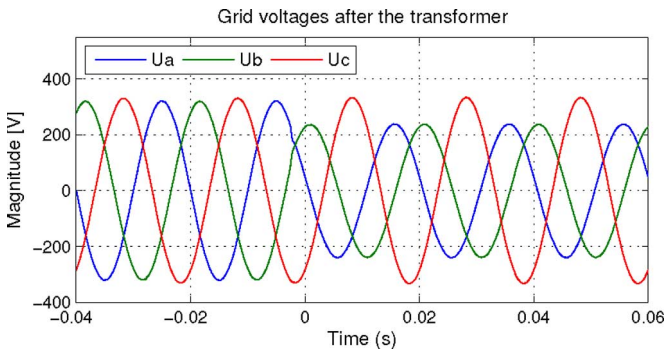

Fig. 10. Voltages at the DPGS terminals in the situation of a single-phase-to-ground fault in the power system.

magnitude at the PCC can be calculated using the voltage divider approach

$$V_{\mathrm{PCC}} = \frac{7700}{10000 + 7700} \cdot 30000 \text{ V}. \tag{26}$$

In this situation, the rms voltage in the faulted line at the secondary of the distribution transformer becomes

$$V_{\mathrm{DPGS}} = \frac{1}{\sqrt{3}} \frac{400}{30000} \cdot V_{\mathrm{PCC}} = 100 \text{ V}. \tag{27}$$

Additionally, the distribution transformer has influence on how the voltages are transferred to the DPGS terminals [9]; therefore, in the situation of this fault, the voltages at the DPGS terminals are behaving as Fig. 10 depicts.

VII. Experimental Results

In order to validate the aforementioned proposed control strategies, the ac power source has been programmed to produce the voltages that are illustrated in Fig. 10 at the terminals of the grid converter in the laboratory. In the following, the grid current as well as the output power waveforms are presented for each control strategy.

A. Instantaneous Active Reactive Control

The current waveforms and the output active and reactive powers for this control strategy are depicted in Fig. 11(a) and (b), respectively. As might be noticed, the current waveforms become very distorted in order to fulfill the demand of the unity power factor control in the situation of an unbalanced

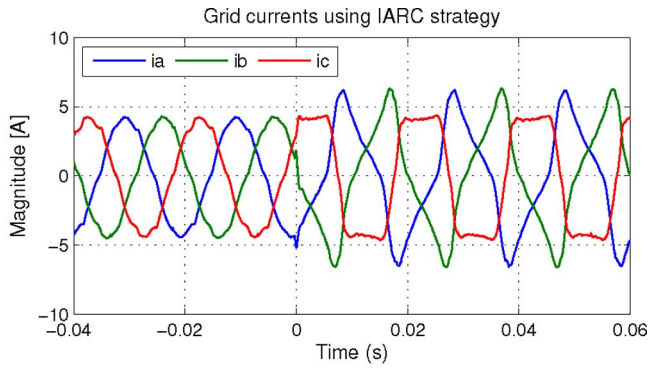

(a)

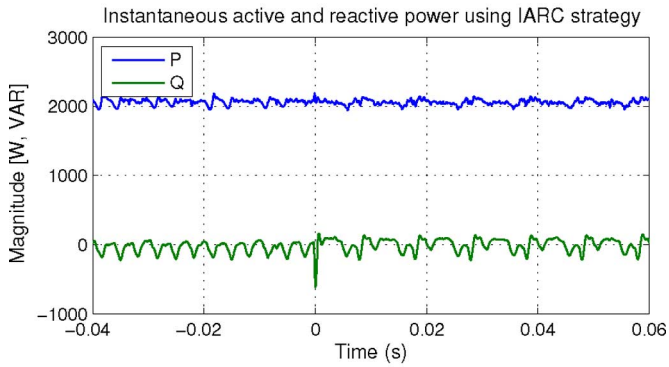

(b)

Fig. 11. Experimental results in the case of a single-phase-to-ground fault using IARC: (a) grid currents and (b) active and reactive powers that are delivered to the utility network.

fault. Additionally, it is difficult to calculate the peak current in this situation due to the nonsinusoidal shape, and it should be noticed here that a high dynamic current controller is necessary in order to have control of the currents in this situation. As mentioned previously in Section IV-A, the instantaneous active and reactive powers that are delivered to the utility network are constant during the fault.

B. Instantaneous Controlled Positive Sequence

The results in the case of the ICPS strategy for the same grid fault, as shown in Fig. 10, are depicted in Fig. 12. As (6) indicates, oscillations at double the fundamental frequency appear in the reactive power using this control strategy, which may be observed in Fig. 11(b). The grid currents are not so highly distorted as in the case of the previous control strategy, but they are still far from being sinusoidal; hence, it is again difficult to estimate the peak current during the fault.

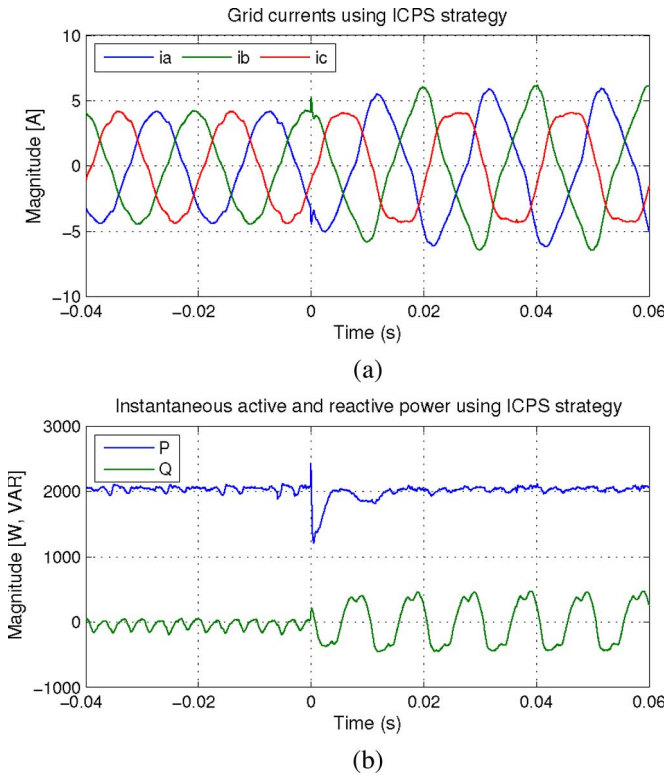

Fig. 12. Experimental results in the case of a single-phase-to-ground fault using ICPS: (a) grid currents and (b) active and reactive powers that are delivered to the utility network.

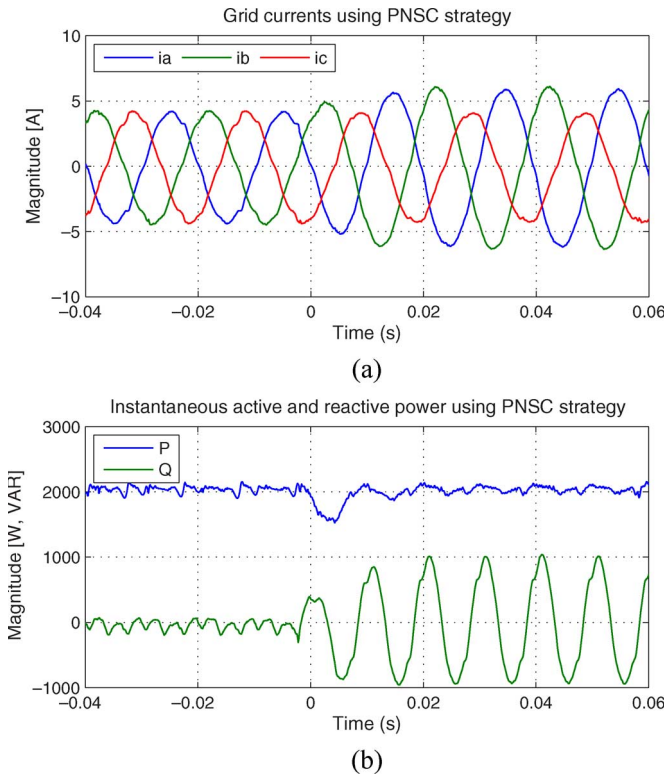

Fig. 13. Experimental results in the case of a single-phase-to-ground fault using PNSC: (a) grid currents and (b) the active and reactive powers that are delivered to the utility network.

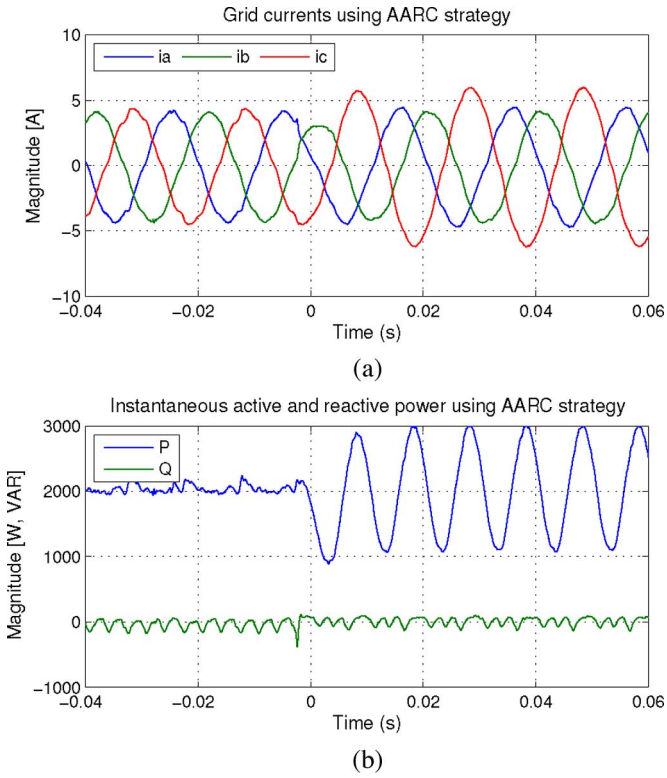

Fig. 14. Experimental results in the case of a single-phase-to-ground fault using AARC: (a) grid currents and (b) active and reactive powers that are delivered to the utility network.

C. Positive–Negative-Sequence Control

Fig. 13 illustrates the grid currents and active and reactive powers that are delivered to the utility grid when PNSC is used. As the meaning of this control is to inject negative-sequence current in order to cancel the oscillations in active power, no oscillations can be observed in the active-power waveform.

The grid currents have a sinusoidal waveform in this case, but they are unbalanced. One advantage of this control is that one can estimate the peak current during the fault as opposed to the two previously discussed strategies. Large oscillations on the reactive-power waveform can be noticed in this situation due to the interaction between the negative-sequence active current with the positive-sequence voltage and the positive-sequence active current with the negative-sequence voltage.

D. Average Active Reactive Control

As opposed to the preceding control strategy, in the case of AARC, the reactive power registers no oscillations, but active power exhibits large oscillations at double the fundamental frequency due to the oscillations in $|\mathbf{v}|^2$ in (15). As shown in Fig. 14, the grid currents are again sinusoidal but unbalanced; moreover, they are monotonously proportional with the voltage since G is a constant in (13).

E. Balanced Positive-Sequence Control

Fig. 15 shows the current and power waveforms in the case of BPSC control. As only the positive-sequence component of the grid voltage is used for calculating the grid current references,

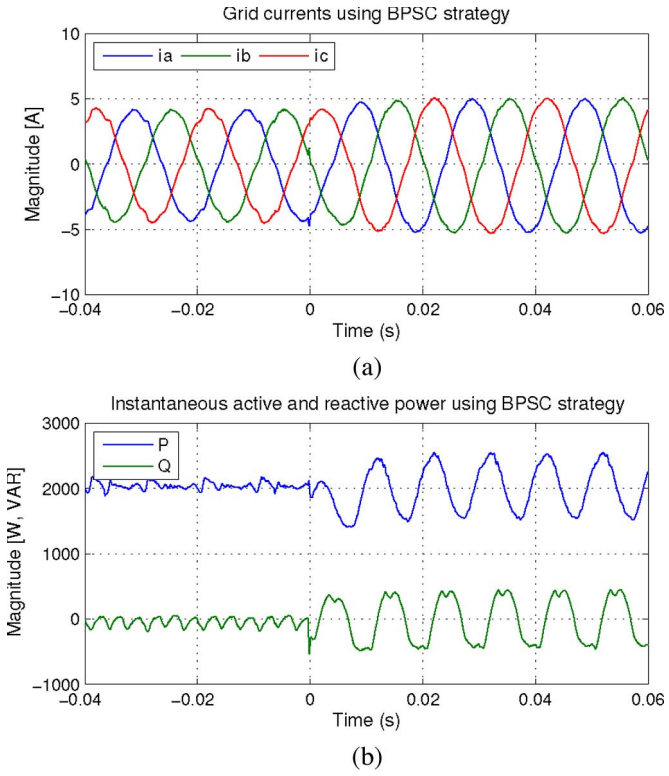

Fig. 15. Experimental results in the case of a single-phase-to-ground fault using BPSC: (a) grid currents and (b) active and reactive powers that are delivered to the utility network.

the currents are sinusoidal and balanced. Noticeable in this case are the oscillations at double the fundamental frequency in both the active and reactive powers, due to the interaction between the positive-sequence current and negative-sequence voltage, as (17) and (18) anticipate.

VIII. Conclusion

The aim of this paper was to investigate several methods that deal with the control of DPGS in the case of unbalance conditions that are caused by faults in the utility grid. The results of the analysis allow for the design of a flexible active power controller that is capable of adapting itself to the fault situation and is reconfigurable in case the grid requirements change. In particular, it has been proven that, during unbalance conditions, it is possible to obtain zero active and reactive power oscillations only by accepting highly distorted currents. However, an intermediate solution allows having sinusoidal grid currents compensating for the oscillation in the active power only, while oscillations are present in the reactive one. It has been proven that the DPGS can be a very flexible power producer that is able to work in constant current, constant active power, or constant reactive power modes depending on the grid fault type and the utility network necessity.

References

[1] F. Blaabjerg, Z. Chen, and S. Kjaer, "Power electronics as efficient interface in dispersed power generation systems," *IEEE Trans. Power Electron.*, vol. 19, no. 5, pp. 1184–1194, Sep. 2004.

[2] J. Carrasco, L. Franquelo, J. Bialasiewicz, E. Galvan, R. PortilloGuisado, M. Prats, J. Leon, and N. Moreno-Alfonso, "Power-electronic systems for the grid integration of renewable energy sources: A survey," *IEEE Trans. Ind. Electron.*, vol. 53, no. 4, pp. 1002–1016, Jun. 2006.

[3] Eltra and Elkraft. (2004). *Wind turbines connected to grids with voltage below 100 kV*. [Online]. Available: http://www.eltra.dk

[4] "Grid code-high and extra high voltage," *E.ON Netz GmbH*, 2006. Tech. Rep. [Online]. Available: http://www.eon-netz.com/Ressources/downloads/ENENARHS2006eng.pdf

[5] R. Cardenas, R. Pena, M. Perez, J. Clare, G. Asher, and P. Wheeler, "Power smoothing using a flywheel driven by a switched reluctance machine," *IEEE Trans. Ind. Electron.*, vol. 53, no. 4, pp. 1086–1093, Jun. 2006.

[6] G. Cimuca, C. Saudemont, B. Robyns, and M. Radulescu, "Control and performance evaluation of a flywheel energy-storage system associated to a variable-speed wind generator," *IEEE Trans. Ind. Electron.*, vol. 53, no. 4, pp. 1074–1085, Jun. 2006.

[7] D. Vilathgamuwa, H. Wijekoon, and S. Choi, "A novel technique to compensate voltage sags in multiline distribution system—The interline dynamic voltage restorer," *IEEE Trans. Ind. Electron.*, vol. 53, no. 5, pp. 1603–1611, Oct. 2006.

[8] M. I. M. Montero, E. R. Cadaval, and F. B. Gonzalez, "Comparison of control strategies for shunt active power filters in three-phase four-wire systems," *IEEE Trans. Power Electron.*, vol. 22, no. 1, pp. 229–236, Jan. 2007.

[9] M. H. J. Bollen, *Understanding Power Quality Problems: Voltage Sags and Interruptions*. Piscataway, NJ: IEEE Press, 2002.

[10] G. Saccomando, J. Svensson, and A. Sannino, "Improving voltage disturbance rejection for variable-speed wind turbines," *IEEE Trans. Energy Convers.*, vol. 17, no. 3, pp. 422–428, Sep. 2002.

[11] L. Moran, P. Ziogas, and G. Joos, "Design aspects of synchronous PWM rectifier-inverter systems under unbalanced input voltage conditions," *IEEE Trans. Ind. Appl.*, vol. 28, no. 6, pp. 1286–1293, Nov./Dec. 1992.

[12] M. Liserre, C. Klumpner, F. Blaabjerg, V. Monopoli, and A. Dell'Aquila, "Evaluation of the ride-through capability of an active-front-end adjustable speed drive under real grid conditions," in *Proc. IECON*, 2004, vol. 2, pp. 1688–1693.

[13] D. Vilathgamuwa, P. Loh, and Y. Li, "Protection of microgrids during utility voltage sags," *IEEE Trans. Ind. Electron.*, vol. 53, no. 5, pp. 1427–1436, Oct. 2006.

[14] M. Prodanovic and T. Green, "High-quality power generation through distributed control of a power park microgrid," *IEEE Trans. Ind. Electron.*, vol. 53, no. 5, pp. 1471–1482, Oct. 2006.

[15] J. Guerrero, J. Matas, L. Garcia De Vicunagarcia De Vicuna, M. Castilla, and J. Miret, "Wireless-control strategy for parallel operation of distributed-generation inverters," *IEEE Trans. Ind. Electron.*, vol. 53, no. 5, pp. 1461–1470, Oct. 2006.

[16] H.-S. Song and K. Nam, "Dual current control scheme for PWM converter under unbalanced input voltage conditions," *IEEE Trans. Ind. Electron.*, vol. 46, no. 5, pp. 953–959, Oct. 1999.

[17] G. Saccomando and J. Svensson, "Transient operation of grid-connected voltage source converter under unbalanced voltage conditions," in *Proc. IAS*, Chicago, IL, 2001, vol. 4, pp. 2419–2424.

[18] A. Sannino, M. Bollen, and J. Svensson, "Voltage tolerance testing of three-phase voltage source converters," *IEEE Trans. Power Del.*, vol. 20, no. 2, pp. 1633–1639, Apr. 2005.

[19] A. Stankovic and T. Lipo, "A novel control method for input output harmonic elimination of the PWM boost type rectifier under unbalanced operating conditions," *IEEE Trans. Power Electron.*, vol. 16, no. 5, pp. 603–611, Sep. 2001.

[20] F. Blaabjerg, R. Teodorescu, M. Liserre, and A. Timbus, "Overview of control and grid synchronization for distributed power generation systems," *IEEE Trans. Ind. Electron.*, vol. 53, no. 5, pp. 1398–1409, Oct. 2006.

[21] H. Akagi, Y. Kanazawa, and A. Nabae, "Instantaneous reactive power compensator comprising switching devices without energy storage components," *IEEE Trans. Ind. Appl.*, vol. IA-20, no. 3, pp. 625–630, 1984.

[22] M. Baumann and J. Kolar, "A novel control concept for reliable operation of a three-phase three-switch buck-type unity-power-factor rectifier with integrated boost output stage under heavily unbalanced mains condition," *IEEE Trans. Ind. Electron.*, vol. 52, no. 2, pp. 399–409, Apr. 2005.

[23] M. Depenbrock, V. Staudt, and H. Wrede, "A theoretical investigation of original and modified instantaneous power theory applied to four-wire systems," *IEEE Trans. Ind. Appl.*, vol. 39, no. 4, pp. 1160–1168, Jul./Aug. 2003.

[24] P. Rodriguez, R. Teodorescu, I. Candela, A. V. Timbus, and F. Blaabjerg, "New positive-sequence voltage detector for grid synchronization of power converters under faulty grid conditions," in *Proc. PESC*, 2006, pp. 1–7.

[25] P. Rodriguez, A. V. Timbus, R. Teodorescu, M. Liserre, and F. Blaabjerg, "Independent PQ control for distributed power generation systems under grid faults," in *Proc. IECON*, 2006, pp. 5185–5190.

Pedro Rodriguez (S'99–M'04) received the B.S. degree in electrical engineering from the University of Granada, Granada, Spain, in 1989 and the M.S. and Ph.D. degrees in electrical engineering from the Technical University of Catalonia (UPC), Barcelona, Spain, in 1994 and 2004, respectively.

In 1990, he joined the faculty of UPC as an Assistant Professor and became an Associate Professor in 1993. He was a Researcher in the Center for Power Electronics Systems, Virginia Polytechnic Institute and State University, Blacksburg, and in the Institute of Energy Technology, Aalborg University, Aalborg, Denmark, in 2005 and 2006, respectively. He is currently the Head of the Research Group on Renewable Electrical Energy Systems, Department of Electrical Engineering, UPC. His research interests include power conditioning, integration of distributed energy systems, and control of power converters.

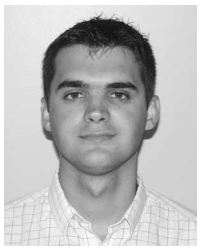

Adrian V. Timbus (S'04) received the Engineer Diploma and the Master degree from Technical University of Cluj, Cluj-Napoca, Romania, in 2000 and 2001, respectively, and the M.Sc.EE. degree from Aalborg University, Aalborg, Denmark, in 2003. He is currently working toward the Ph.D. degree at the Institute of Energy Technology, Aalborg University.

His research interests include control of power converters, particularly, when employed for renewable energy systems; advanced control in order to overcome grid faults, and grid synchronization and grid monitoring.

Mr. Timbus is a member of the IEEE Power Electronics Society, IEEE Industrial Electronics Society, and IEEE Power Engineering Society.

Remus Teodorescu (S'96–A'97–M'99–SM'02) received the Dipl.Ing. degree in electrical engineering from Polytechnical University of Bucharest, Bucharest, Romania, in 1989 and the Ph.D. degree in power electronics from the University of Galati, Galati, Romania, in 1994.

From 1989 to 1990, he was with Iron and Steel Plant Galati. He then moved to the Department of Electrical Engineering, University of Galati, where he was an Assistant and has been an Assistant Professor since 1994. In 1996, he was appointed Head of the Power Electronics Research Group, University of Galati. In 1998, he joined the Power Electronics and Drives Department, Institute of Energy Technology, Aalborg University, Aalborg, Denmark, where he is currently an Associate Professor. He has published more than 60 papers and one book. He is the holder of two patents. His research interests include power converters for renewable energy systems, solar cells, multilevel inverters, digital control, and computer simulations of advanced electrical drives.

Dr. Teodorescu is a corecipient of the Technical Committee Prize Paper Awards at IEEE-IAS'98 and the OPTIM-ABB Prize Paper Award at OPTIM 2002.

Marco Liserre (S'00–M'03–SM'07) received the M.Sc. and Ph.D. degrees in electrical engineering from Politecnico di Bari, Bari, Italy, in 1998 and 2002, respectively.

He is currently an Assistant Professor in the Department of Electrotechnical and Electronic Engineering, Politecnico di Bari. He has coauthored some 100 technical papers; 20 of them have been published or are to be published in peer-reviewed international journals. He is a coauthor of three chapters of the book that was edited by F. Lattarulo titled *Electromagnetic Compatibility in Power Systems* (Elsevier, 2006). His research interests are focused on industrial electronics applications to distributed power generation systems based on renewable energies.

Dr. Liserre is a member of the IEEE Industry Applications, IEEE Industrial Electronics, and IEEE Power Electronics Societies. In the IEEE Industrial Electronics Society, he was an AdCom Member in the period 2003–2004, Chair for Student Activities in the period 2002–2004, Chair for Region 8 Membership Activities in 2004, and Newsletter Editor in 2005. He is an Associate Editor of the IEEE TRANSACTION ON INDUSTRIAL ELECTRONICS. He is Editor-in-Chief of the new *IEEE Industrial Electronics Magazine*.

Frede Blaabjerg (S'90–M'91–SM'97–F'03) received the M.Sc.EE. degree from Aalborg University, Aalborg, Denmark, in 1987 and the Ph.D. degree from the Institute of Energy Technology, Aalborg University, in 1995.

From 1987 to 1988, he was with ABB-Scandia, Randers, Denmark. During 1988–1992, he was a Ph.D. student at the Institute of Energy Technology, Aalborg University, where he became an Assistant Professor in 1992, an Associate Professor in 1996, a Full Professor in power electronics and drives in 1998, and the Dean of Faculty of Engineering and Science in 2006. He is the author or coauthor of more than 300 publications in his research fields including the book *Control in Power Electronics* (Academic, 2002). During the last years, he has held a number of chairman positions in research policy and research funding bodies in Denmark. His research areas are power electronics, static power converters, ac drives, switched reluctance drives, modeling, characterization of power semiconductor devices and simulation, wind turbines, and green power inverters.

Dr. Blaabjerg is an Associate Editor of the IEEE TRANSACTIONS ON INDUSTRY APPLICATIONS, IEEE TRANSACTIONS ON POWER ELECTRONICS, *Journal of Power Electronics* and the Danish journal *Elteknik*. In 2006, he became the Editor in Chief of the IEEE TRANSACTIONS ON POWER ELECTRONICS. He was the recipient of the 1995 Angelos Award for his contribution in modulation technique and control of electric drives; the Annual Teacher Prize at Aalborg University in 1995; the Outstanding Young Power Electronics Engineer Award from the IEEE Power Electronics Society in 1998; five IEEE Prize Paper Awards during the last six years; the C.Y. O'Connor Fellowship 2002 from Perth, Australia; the Statoil-Prize for his contributions in power electronics in 2003, and the Grundfos-Prize for his contributions in power electronics and drives in 2004.